Crystallographic alignment of high-density gallium nitride nanowire arrays

TEVYE KUYKENDALL[1]*, PETER J. PAUZAUSKIE[1]*, YANFENG ZHANG[2], JOSHUA GOLDBERGER[1], DONALD SIRBULY[2], JONATHAN DENLINGER[3] AND PEIDONG YANG[1,2]†

[1]Department of Chemistry, University of California, Berkeley, California 94720, USA
[2]Materials Science Division, Lawrence Berkeley National Laboratory, Berkeley, California 94720, USA
[3]Advanced Light Source, Lawrence Berkeley National Laboratory, Berkeley, California 94720, USA
*These authors contributed equally to this work
†e-mail: p_yang@uclink.berkeley.edu

Published online: 25 July 2004; doi:10.1038/nmat1177

Single-crystalline, one-dimensional semiconductor nanostructures are considered to be one of the critical building blocks for nanoscale optoelectronics[1]. Elucidation of the vapour–liquid–solid growth mechanism[2] has already enabled precise control over nanowire position and size[1,3,4–8], yet to date, no reports have demonstrated the ability to choose from different crystallographic growth directions of a nanowire array. Control over the nanowire growth direction is extremely desirable, in that anisotropic parameters such as thermal and electrical conductivity, index of refraction, piezoelectric polarization, and bandgap may be used to tune the physical properties of nanowires made from a given material. Here we demonstrate the use of metal–organic chemical vapour deposition (MOCVD) and appropriate substrate selection to control the crystallographic growth directions of high-density arrays of gallium nitride nanowires with distinct geometric and physical properties. Epitaxial growth of wurtzite gallium nitride on (100) γ-$LiAlO_2$ and (111) MgO single-crystal substrates resulted in the selective growth of nanowires in the orthogonal [1$\bar{1}$0] and [001] directions, exhibiting triangular and hexagonal cross-sections and drastically different optical emission. The MOCVD process is entirely compatible with the current GaN thin-film technology, which would lead to easy scale-up and device integration.

Gallium nitride is a wide-bandgap semiconductor and a prime candidate for use in future high-performance, high-power optoelectronic devices because of its high melting point, carrier mobility, and electrical breakdown field. Single-crystalline gallium nitride nanowires[9] and nanotubes[10] have already shown promise for realizing photonic and biological nanodevices such as blue light-emitting diodes[11], short-wavelength ultraviolet nanolasers[6,12], and nanofluidic biochemical sensors. Almost all reported synthetic schemes for GaN-based materials to date have used either laser ablation[13], chemical vapour transport[6,8,9,14–16] or hydride vapour epitaxy and molecular beam epitaxy[17–19]. Most of these processes use Ga metal as the vapour source. Metals such as Ni, Fe and Au have been used as initiators for vapour–liquid–solid (VLS) nanowire growth[5–12,20]. Previously, we reported the synthesis and characterization of GaN nanowires using a metal-initiated MOCVD process[21]. Trimethylgallium and ammonia source materials were used as Ga and N precursors.

The selection of single-crystal substrates is critical for achieving deterministic control of growth direction. A close match of both symmetry and lattice constant between the substrate and GaN is essential for successful heteroepitaxy, and is anticipated to influence strongly the nanowire growth direction. The oxygen sublattice in the (100) plane of γ-$LiAlO_2$ has twofold symmetry, which matches well with the twofold symmetry of the (100) plane of wurtzite GaN. The lattice constants a = 5.17 Å and c = 6.28 Å of γ-$LiAlO_2$ match closely to the lattice constants c = 5.19 Å and two times a = 3.19 Å of GaN, respectively. In contrast, the (111) plane of MgO has threefold symmetry and an interatomic separation of 2.98 Å for atoms in the (111) plane. This matches well with the threefold symmetry of the (001) plane of GaN and the lattice constant a = 3.19 Å. As a result, we chose these two substrates with the expectation of selectively growing GaN nanowires with [1$\bar{1}$0] and [001] directions, respectively.

Field-emission scanning electron microscopy (FE-SEM; FEI-235) was used to investigate the nanowire length, shape and overall substrate coverage. Figure 1a shows an overview of the GaN nanowire coverage on a patterned, gold-coated γ-$LiAlO_2$ (100) substrate. There are several important features for these GaN nanowires (Fig. 1 a–c). First, the nanowires grow perpendicular to the substrate. Second, as a result of the VLS growth, the nanowires grow only in areas with Au thin-film coating, which readily yields patterned nanowires as seen in the figure. This selective growth capability would be very helpful for future nanowire device integration. Third, all nanowires exhibit symmetry-matched isosceles cross-sections. The widths, measured along the base of the triangles, are 15–40 nm and the lengths measure from 1–5 μm. Longer wires, with similar widths have also been achieved by using longer growth times. Significantly, the in-plane crystallographic alignment of these nanowires is apparent (Fig. 1c). Note that the in-plane C_2-rotation axis for the isosceles triangles (parallel with the c axis of GaN) is always parallel with the in-plane [010] direction for γ-$LiAlO_2$; this is because of the excellent symmetry and lattice match between the wire and substrate crystal structures.

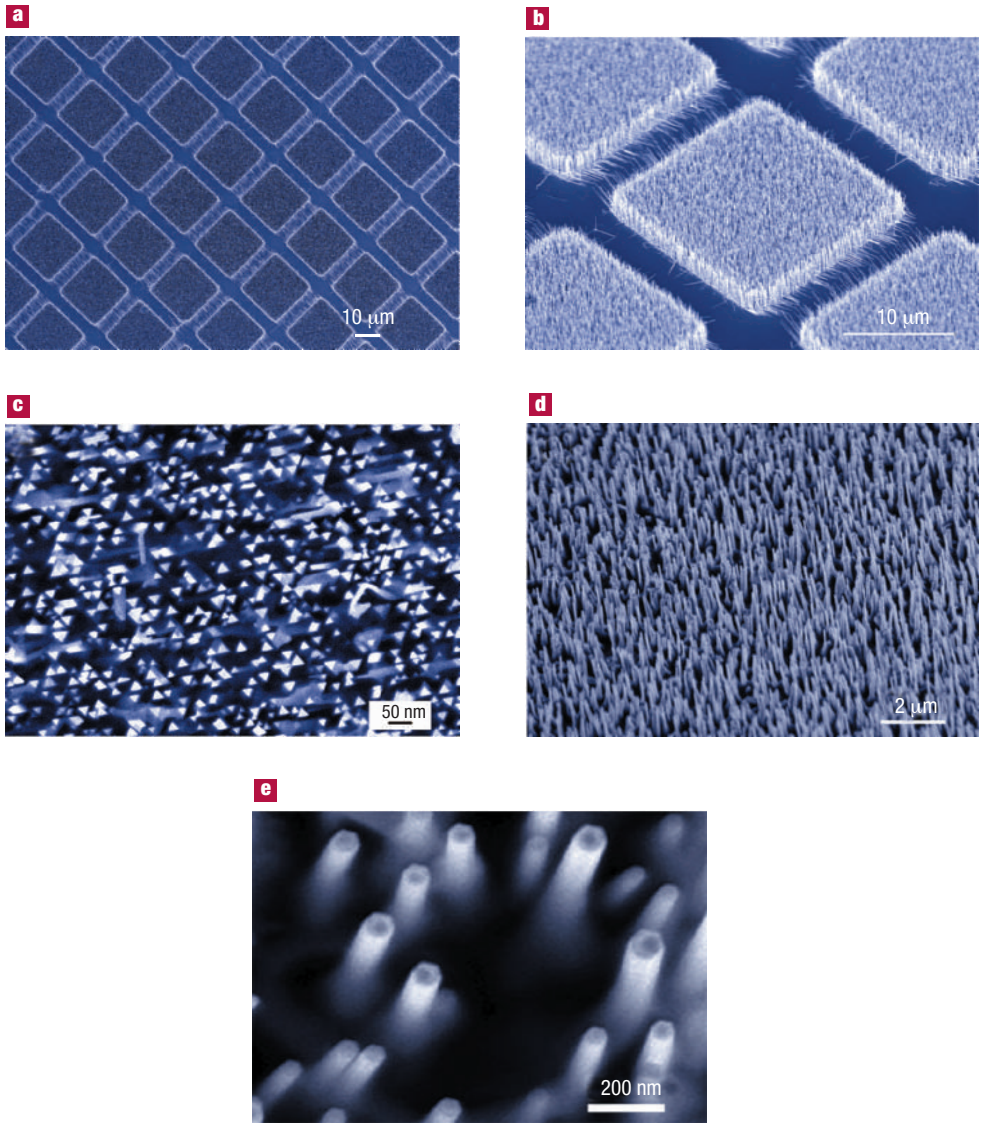

Figure 1 SEM images of the GaN nanowires. a–c, Wires grown on (100) γ-$LiAlO_2$. **d–e**, Wires grown on (111) MgO substrates.

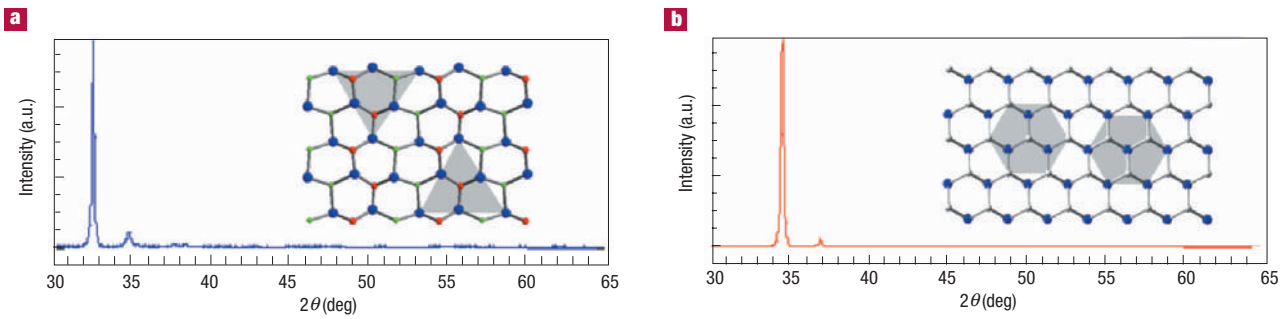

Figure 2 XRD patterns. a, The (100) peak corresponds to the orthogonal [1$\bar{1}$0] growth direction. **b**, The (002) peak corresponds to the orthogonal [001] growth direction. The insets show the crystal structures of the substrate at the interface between the substrate and the wire that dictate the selective GaN nanowire growth. Inset in **a**: $LiAlO_2$: Li (green), Al (red), O (blue). Inset in **b**: MgO: Mg (grey), O (blue). The grey boxes indicate the respective orientation of the GaN crystal planes at the interface. a.u. = arbitrary units.

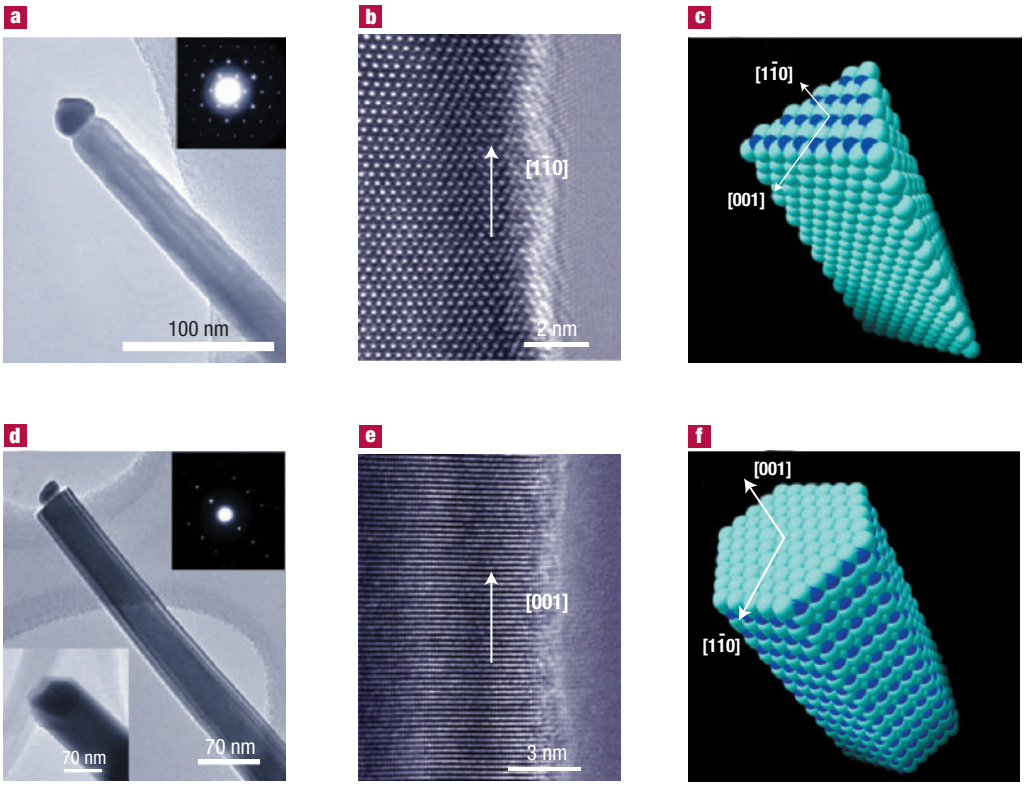

Figure 3 TEM images of the GaN nanowires. a–c, Wires grown on (100) γ-$LiAlO_2$. The inset in **a** is an electron-diffraction pattern recorded along [001] zone axis. **d–f**, Wires grown on (111) MgO substrates. The insets in **d** show the hexagonal cross-section of the wire and an electron-diffraction pattern recorded along the [1$\bar{1}$0] zone axis. **c** and **f** show space-filling structural models for the nanowires with triangular and hexagonal cross-sections.

X-ray diffraction (XRD; Siemens D5000) recorded on the nanowire arrays grown on γ-$LiAlO_2$ shows almost exclusively (100) diffraction (Fig. 2a), a clear indication that the nanowires grow perfectly along the [1$\bar{1}$0] direction. These nanowires were dispersed on transmission electron microscopy (TEM; Philips CM200 FEG) grids in order to carry out additional structural and compositional analysis. Figure 3a shows a TEM image of an individual GaN nanowire, where a metal droplet can be clearly seen on its tip. The composition of the Au metal tip was confirmed with energy-dispersive X-ray spectroscopy. Analysis of the electron-diffraction pattern (inset) taken along the [001] zone axis indicates that the nanowire grows in the [1$\bar{1}$0] direction, perpendicular to (100) crystal plane. Figure 3b shows a high-resolution TEM image of the nanowire, showing exactly the (100) lattice plane perpendicular to the wire axis. In addition, electron-energy-loss spectroscopy analysis clearly showed a nitrogen peak and the absence of an oxygen peak, confirming the compositional purity of the nanowires. Our previous TEM studies on [1$\bar{1}$0]-oriented GaN nanowires indicate that these triangular cross-sections are not equilateral[21], that is, the observation of these triangular cross-sections is not a result of viewing along the sixfold crystallographic symmetry axis (*c* axis). Instead, the isosceles triangular cross-section is a manifestation of the twofold symmetry along the [1$\bar{1}$0] crystallographic direction, and the nanowires are enclosed by the (112), ($\bar{1}\bar{1}$2) and (001) side planes (Fig. 3c).

Interestingly, when (111) MgO was used as the substrate under nearly identical synthetic conditions, similar vertically aligned GaN nanowire arrays were obtained (Fig. 1d,e), but with the orthogonal [001] growth direction. The nanowires have an overall similar dimension to those wires grown on $LiAlO_2$ substrates, except that every wire has a hexagonal cross-section. Again, all of these hexagonal wires exhibit excellent in-plane crystallographic alignment resulting from the symmetry and lattice match at the interface. Figure 2b shows XRD for these wires. In contrast to the wires grown on (100) γ-$LiAlO_2$ substrates, the XRD exhibits only (002) diffraction, indicating that the wires grow along the [001] direction. This is further confirmed by TEM characterization. Figure 3d,e shows TEM images and an electron-diffraction pattern recorded on these nanowires. The (001) lattice fringe can readily be seen in Fig. 3e as well as a hexagonal cross-section in Fig. 3d, lower inset. TEM analysis of these nanowires clearly indicates that they grow along the [001] direction and are enclosed by {100} side planes (Fig. 3f).

In addition to demonstrating the controlled growth of vertically aligned GaN nanowires in the [001] and [1$\bar{1}$0] orientations, we have also achieved similar control over the orientation of ZnO nanostructures. Previously, when a-plane sapphire was used as the substrate, vertical hexagonal ZnO nanowire arrays were produced[22,23]. Owing to the close match between lattice parameters of GaN and ZnO, similar results to those achieved for GaN were expected. In fact, when $LiAlO_2$ was used as the substrate for ZnO growth, ZnO nanoribbon arrays with [1$\bar{1}$0] vertical alignment have been achieved (see Supplementary Information). Rectangular, as opposed to triangular, cross-sections are observed for the ZnO arrays, probably due to the different polarity and surface energies for GaN and ZnO crystals (See Supplementary Information).

Being able to control the nanowire growth direction represents one significant step towards tuning material properties through rational nanostructure synthesis, as the optical and electrical properties of the

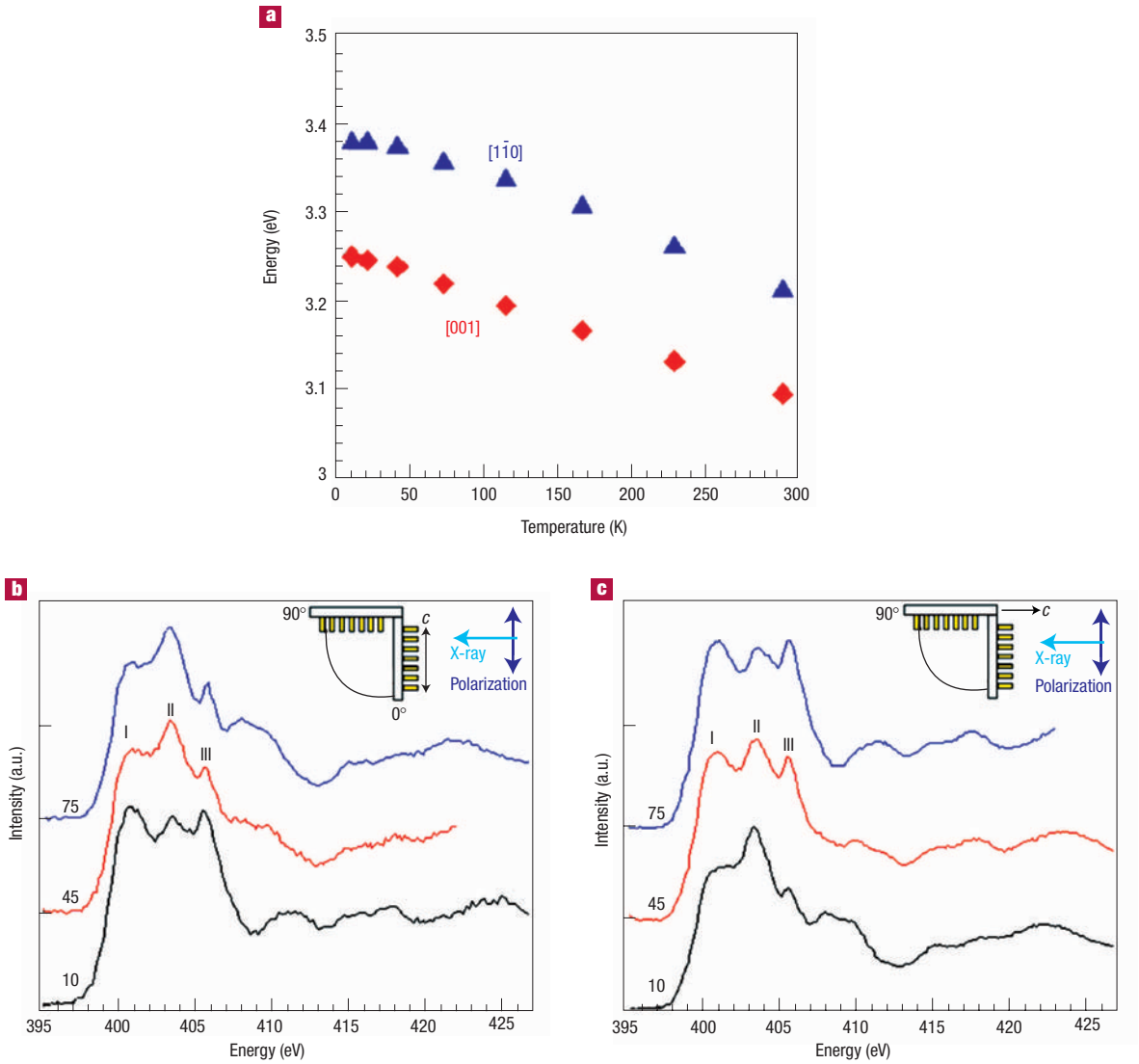

Figure 4 Photoluminescence spectra and polarized XAS. a, Temperature-dependent photoluminescence collected on the two sets of GaN nanowires with different growth directions. The emission energy is plotted as a function of the temperature. **b**, XAS spectra for [1$\bar{1}$0] wires showing the N K-edge absorption as the array sample rotates with respect to the polarization. **c**, XAS spectra for [001] wires showing the N K-edge absorption as the array sample rotates with respect to the polarization. In both **a** and **b**, the numbers 10, 45 and 75 refers to the sample rotation angle; the insets show the sample rotation configuration with the *c* axis in the plane of the incident photon polarization; I and III refer to the final p_z states and II to the final p_{xy} states.

anisotropic nanostructures often depend not only on their dimensions, but on their crystallographic orientations as well[24]. To demonstrate such an orientation-induced effect, temperature-dependent photoluminescence studies were carried out and emissions from these two types of samples were compared. Figure 4 shows a clear difference in the optical emission from these two different arrays at temperatures ranging from 5 K to 285 K. In general, the emission for the [1$\bar{1}$0] wires is blue-shifted by ~100 meV from that of [001] wires. As these two sets of wires have similar diameter distributions, we believe that the emission difference is a clear manifestation of the different wurtzite growth directions. In particular, the [001] and [1$\bar{1}$0] directions represent two orthogonal crystallographic orientations within the wurtzite GaN crystal structure, the first polar and the other non-polar. It has been shown that the presence of spontaneous polarization in GaN has a drastic impact on electron–hole overlap, radiative lifetimes, and subsequent emission wavelength and quantum efficiencies for GaN (ref. 25). In addition, the difference in tensile stress and defects experienced by wires grown along different directions could also contribute to this emission difference[15]. Finally, the unique isosceles triangle cross-section of the [1$\bar{1}$0] wires might also lead to interesting carrier-confinement effects at the triangle vertices, which could contribute to the blue-shifting of photoluminescence.

Furthermore, significant anisotropy in the valence band is expected for wurtzite nanostructures[26], especially for these anisotropic nanostructures. The nitrogen partial density of states in the conduction band in these two sets of samples has been probed by polarized X-ray absorption spectroscopy (XAS)[27,28]. The XAS studies are orbital-symmetry specific, orientation dependent, and capable of projecting

conduction states separately along specific crystallographic directions (See Methods). In our XAS experiments, sample rotation allowed the incident beam angle to be varied from near-normal incidence (10°) to near-grazing (75°), thus varying the polarization **e**-vector from perpendicular to near-parallel to the nanowire axis, respectively (Fig. 4b,c insets). Absorption of the [1$\bar{1}$0] nanowire arrays showed a strong dependence on the angle of incidence with the *c* axis near-normal to **e** at 75° and near-parallel at 10° (Fig. 4b). The [001] array absorption spectra also showed similar strong angular dependence (Fig. 4c) with the *c* axis near-normal to **e** at 10° and near-parallel at 75°, only with the intensity trend reversed as the result of the two orthogonal crystallographic directions in our samples. The dependence of our XAS spectra on array orientation agrees strongly with the above XRD and SEM data, unambiguously showing that these arrays exhibit excellent crystallographic alignment as well as significant anisotropy in morphology and electronic structure.

METHODS

MATERIAL SYNTHESIS

In general, a 2–3 nm thin film of Ni, Fe or Au catalyst was thermally evaporated onto the substrates. For patterned nanowire growth, a TEM grid is used as a shadow mask during metal deposition. Subsequent VLS growth of GaN nanowires occurred at a substrate temperature of 900 °C in a hot-wall CVD system. The reaction was carried out in an oxygen-free environment at atmospheric pressure. Trimethylgallium (Aldrich) was kept cool in a bath at –10 °C. Nitrogen, used as a carrier gas, was percolated through the trimethylgallium precursor and coupled with a second nitrogen line to give a total nitrogen flow rate of 250 s.c.c.m. These were supplied by a 4 mm ID quartz tube. Hydrogen and ammonia sources were supplied by a 22 mm ID outer quartz tube at a total flow rate of ~155 s.c.c.m. Wire coverage was obtained on substrates placed from 1 to 10 cm away from the organic precursor outlet. The deposition generally took 5–30 minutes.

OPTICAL CHARACTERIZATION

Photoluminescence of the nanowires was collected at different temperatures within an optical cryostat (Janis ST-100). The sample was excited with the 325 nm line of a He–Cd continuous-wave laser (Omnichrome 2074-S-A01). The nanowire emission was collected, dispersed with a 0.3 m monochromator and detected by an intensified charge-coupled detector (Princeton Instruments Spec 10-100B).

POLARIZED XAS

The nitrogen partial density of states in the conduction band was probed by XAS with undulator beamline 8.0 at the Advanced Light Source of the Lawrence Berkeley National Laboratory. Linearly polarized soft X-rays were tuned to the nitrogen K-edge ranging between 395 and 430 eV, with a spot size of roughly 0.1 × 1.0 mm and resolution ~0.2 eV. Total fluorescence-yield absorption was measured using the signal from a channeltron, biased for detection of emitted photons, recorded as function of photon energy and incidence angle.

The angular dependence observed in XAS experiments can be explained by the large degree of electronic anisotropy in wurtzite's non-centrosymmetric crystal structure. This has been demonstrated previously with polarized synchrotron radiation through analysis of cubic and hexagonal GaN thin films, and of polycrystalline GaN powders[27,28]. Photon absorption depends on the matrix element $M = \langle\phi_{1s}|\mathbf{e}\cdot\mathbf{r}|\phi_f\rangle$ where **e** is the polarization vector of the incoming photon, **r** is the position vector of the electron relative to the nitrogen nucleus, and $\phi_{1s,f}$ are the initial and final state wavefunctions of the nitrogen core electron.

In the wurtzite lattice, XAS spectra depend on the excitation of the two distinct π and σ modes of bonding, with symmetrically distinct **r** position vectors. The π mode occurs along the *c* axis (having C_3 symmetry) and contains a large amount of nitrogen-p_z character. The σ mode makes up the three remaining low-symmetry bonds of the GaN pseudo-tetrahedron[27], forming a σ plane with a large amount of nitrogen-p_{xy} character. Transition of the 1*s* electron to the final p_z states (peak I, III in Fig. 4b,c) is forbidden if the polarization of the photon is perpendicular to the *c* axis, whereas transition to the final p_{xy} states (peak II in Fig. 4b,c) is forbidden if the polarization is parallel to the *c* axis.

Received 6 April 2004; accepted 2 June 2004; published 25 July 2004.

References

1. Xia, Y. *et al.* One-dimensional nanostructures: Synthesis, characterization, and applications. *Adv. Mater.* **15,** 353–389 (2003).
2. Wu, Y. & Yang, P. Direct observation of vapor-liquid-solid nanowire growth. *J. Am. Chem. Soc.* **123,** 3165–3166 (2001).
3. Wu, Y., Yan, H. & Yang, P. Inorganic semiconductor nanowires: Rational growth, assembly, and novel properties. *Chem. Eur. J.* **8,** 1261–1268 (2002).
4. Haraguchi, K. *et al.* Self-organized fabrication of planar GaAs nanowhisker arrays. *Appl. Phys. Lett.* **69,** 386–387 (1996).
5. Han, S. *et al.* Controlled growth of gallium nitride single-crystal nanowires using a chemical vapor deposition method. *J. Mater. Res.* **18,** 245–249 (2003).
6. Holmes, J. D. *et al.* Control of thickness and orientation of solution-grown silicon nanowires. *Science* **287,** 1471–1473 (2000).
7. Ohlsson, B. J., Björk, M. T., Magnusson, M. H., Deppert, K. & Samuelson, L. Size-, shape-, and position-controlled GaAs nano-whiskers. *Appl Phys. Lett.* **79,** 3335–3337 (2001).
8. Mårtensson, T. *et al.* Nanowire arrays defined by nanoimprint lithography. *Nano Lett.* **4,** 699–702 (2004).
9. Johnson, J. C. *et al.* Single gallium nitride nanowire lasers. *Nature Mater.* **1,** 106–109 (2002).
10. Goldberger, J. *et al.* Single-crystal gallium nitride nanotubes. *Nature* **422,** 599–602 (2003).
11. Huang, Y., Duan, X., Cui, Y. & Lieber, C. M. Gallium nitride nanowire nanodevices. *Nano Lett.* **2,** 101–104 (2002).
12. Choi, H. *et al.* Self-organized GaN quantum wire UV lasers. *J. Phys. Chem.* **107,** 8721–8725 (2003).
13. Duan, X. & Lieber, C. M. Laser-assisted catalytic growth of single crystal GaN nanowires. *J. Am. Chem. Soc.* **122,** 188–189 (2000).
14. Chen, C. *et al.* Catalytic growth and characterization of gallium nitride nanowires. *J. Am. Chem. Soc.* **123,** 2791–2798 (2001).
15. Seo, H. *et al.* Strained gallium nitride nanowires. *J. Chem. Phys.* **116,** 9492–9499 (2002).
16. Zhong, Z., Qian, F., Wang, D. & Lieber, C. M. Synthesis of p-type gallium nitride nanowires for electronic and photonic nanodevices. *Nano Lett.* **3,** 343–345 (2003).
17. Kim, H., Kang, T. & Chung, K. Nanoscale ultraviolet-light-emitting diodes using wide-bandgap gallium nitride nanorods. *Adv. Mater.* **15,** 567–569 (2003).
18. Ristic, J. *et al.* AlGaN nanocolumns grown by molecular beam epitaxy: optical and structural characterization. *Phys. Status Solidi A* **192,** 60–66 (2002).
19. Ristic, J. *et al.* Characterization of GaN quantum discs embedded in $Al_xGa_{1-x}N$ nanoclolumns grown by molecular beam epitaxy. *Phys. Rev. B* **68,** 125305 (2003).
20. Stach, E., Pauzauskie, P., Kuykendall, T., Goldberger, J. & Yang, P. Watching GaN nanowires grow. *Nano Lett.* **3,** 867–869 (2003).
21. Kuykendall, T., Pauzauskie, P., Lee, S. K., Zhang, Y. & Yang, P. Metalorganic chemical vapor deposition route to GaN nanowires with triangular cross sections. *Nano Lett.* **3,** 1063–1066 (2003).
22. Huang, M. *et al.* Room-temperature ultraviolet nanowire nanolasers. *Science* **292,** 1897–1899 (2001).
23. Park, W. I., Yi, G., Kim, M. & Pennucook, S. Quantum confinement observed in ZnO/ZnMgO nanorod heterojunctions. *Adv. Mater.* **15,** 526–529 (2003).
24. Bir, G. L. & Pikus, G. E. *Symmetry and Strain-induced Effects in Semiconductors* (Wiley, New York, 1972).
25. Waltereit, P. *et al.* Nitride semiconductors free of electrostatic fields for efficient white light-emitting diodes. *Nature* **406,** 865–868 (2000).
26. Domen, K., Horino, K., Kuramata, A. & Tanahashi, T. Analysis of polarization anisotropy along the c axis in the photoluminescence of wurtzite GaN. *Appl. Phys. Lett.* **71,** 1996–1998 (1997).
27. Lawniczak-Jablonska, K. *et al.* Anisotropy of the nitrogen conduction states in the group III nitrides studied by polarized x-ray absorption spectroscopy. *Appl. Phys. Lett.* **70,** 2711–2713, (1997).
28. Lawniczak-Jablonska, K. *et al.* Electronic states in valence and conduction bands of group-III nitrides: Experiment and theory. *Phys. Rev. B* **61,** 16623–16632 (2000).

Acknowledgements

This work was supported by the Camille and Henry Dreyfus Foundation, Beckman Foundation, the National Science Foundation (CAREER, NIRT) and Department of Energy. P. Y. is an Alfred P. Sloan Research Fellow. P. P. and J. G. thank the National Science Foundation for predoctoral fellowship support. Work at the Lawrence Berkeley National Laboratory was supported by the Office of Science, Basic Energy Sciences, Division of Materials Science of the US Department of Energy. We thank the National Center for Electron Microscopy for the use of their facilities.
Correspondence and requests for materials should be addressed to P.Y.
Supplementary Information accompanies the paper on www.nature.com/naturematerials

Competing financial interests

The authors declare that they have no competing financial interests.